Arabian Journal of Chemistry (2020) 13, 8092–8099

King Saud University

Arabian Journal of Chemistry

www.ksu.edu.sa
www.sciencedirect.com

ORIGINAL ARTICLE

Biocarbonation: A novel method for synthesizing nano-zinc/zirconium carbonates and oxides

Hamdy A. Abdel-Gawwad [a,*], Alaa A. Saleh [a], Pawel Sikora [b,c], Mohamed Abd Elrahman [d], Mona S. Mohammed [e], Hala S. Hussein [e], Essam Nabih Ads [f]

[a] *Raw Building Materials and Processing Technology Research Institute, Housing and Building National Research Center (HBRC), Cairo, Egypt*
[b] *Building Materials and Construction Chemistry, Technische Universität Berlin, Germany*
[c] *Faculty of Civil and Environmental Engineering, West Pomeranian University of Technology Szczecin, Szczecin, Poland*
[d] *Structural Engineering Department, Faculty of Engineering, Mansoura University, Elgomhouria St., Mansoura City 35516, Egypt*
[e] *Department of Chemical Engineering and Pilot Plant, National Research Centre, Cairo, Egypt*
[f] *Faculty of Science, Zagazig University, Zagazig, Egypt*

Received 17 July 2020; accepted 21 September 2020
Available online 1 October 2020

KEYWORDS

Nanoparticles;
Crystal structure;
Microstructure;
Biomaterials;
Urease enzyme-urea;
Nano-sheets

Abstract It is well known that the chemical precipitation is regarded as an effective approach for the preparation of nano-materials. Nevertheless, it represented several drawbacks, including high energy demand, high cost, and high toxicity. This work investigated the eco-sustainable application of plant-derived urease enzyme (PDUE)-urea mixture for synthesizing Zn–/Zr–carbonates and –oxides nanoparticles. Hydrozincite nanosheets and spherical-shaped Zr-carbonate nano-particles were produced after adding PDUE-urea mixture to the dissolved Zn and Zr salts, respectively. PDUE not only acts as a motivator for urea hydrolysis, but it is also used as a dispersing agent for the precipitated nano-carbonates. The exposure of these carbonates to 500 °C for 2 h has resulted in the production of the relevant oxides. The retention time (after mixing urea with urease enzyme) is the dominant parameter which positively affects the yield% of the nano-materials, as confirmed by statistical analyses. Compared with traditional chemical-precipitation, the proposed method exhibited higher efficiency in the formation of nano-materials with smaller particle size and higher homogeneity.

* Corresponding author.
E-mail address: hamdyabdelgawwad@yahoo.com (H.A. Abdel-Gawwad).

Peer review under responsibility of King Saud University.

ELSEVIER Production and hosting by Elsevier

1. Introduction

The high performance of nano-sized materials is the wise reason behind their effective usage in different applications. Zinc and zirconium oxides (ZnO and ZrO_2, respectively) nano-particles represent promising results in many industrial fields (Shamsipur et al., 2013; Maruthupandy et al., 2017; Hafez

https://doi.org/10.1016/j.arabjc.2020.09.040
1878-5352

et al., 2020; Zhan et al., 2020). Traditional chemical-precipitation method is one of the common and effective approaches for preparing nano-ZnO and –ZrO_2 (Singh and Dutta, 2019; Yao et al., 2020). Nevertheless, it exhibited many shortcomings including high toxicity, high energy demand, and high processing cost caused by the high demand of such method for external stabilizing, promoted and base additives during its reaction (Maruthupandy et al., 2017).

Eco-friendly biological methods have been applied to resolve these problems as they are characterized by simplicity, low energy consumption and man power with no advanced equipment's requirements (Hulkoti and Taranath, 2014). Using plants' extracts, such as *Calotropisgigantea, Hibiscus subdariffa, Azadirachta indica, Camellia japonica, Euclea natalensis*, and *Aloevera*, is considered as one of the successful biological methods for synthesizing ZnO and ZrO_2 nano-particles (Maruthupandy et al., 2017; Gowri et al., 2014; da Silva et al., 2019). The reduction reaction is the key feature of these extracts in the formation of nano-oxides. This reaction was performed by the transformation of enol-groups within biomolecule-containing-extracts to keto form, resulting in creating reactive hydrogen reducing agent. Also these extracts act as stabilizing and capping agents for the nano-particles which prevent their agglomeration (da Silva et al., 2019).

A homogeneous precipitation method using Zn/Zr slats and urea as precipitating agent was applied to prepare Zn-/Zr-containing-carbonates. These carbonates was exposed to thermal treatment to produce Zn and/or Zr oxides nanoparticles (da Silva et al., 2019; Marinho et al., 2012a, 2012b; Wahab et al., 2008; Mazitova et al., 2019; Devaiah et al., 2018; Alaei et al., 2014). The anion bearing salt strongly influenced on the decomposition temperature, morphology and particle size of the produced nano-oxides (Srikanth and Jeevanandam, 2009). Homogeneous methods was conducted by mixing metal salt solution with the dissolved urea followed by conventional water bath heating or microwave hydrothermal to yield nano metal oxide (Marinho et al., 2012).

In the present work, a homogeneous precipitation method was conducted using a novel biocarbonation method. Urease enzyme extracted from *Canavalia ensiformis* was used instead of heating for hydrolyzing urea. Accordingly, the homogeneous precipitation method was performed via the interaction of carbonate groups resulted from enzymatic urea hydrolysis with metals, yielding nano-Zn/Zr carbonates. Nano-ZnO and -ZrO_2 were prepared by thermal treatment of nano-Zn/Zr carbonates at 500 °C. This perfectly highlights the successful application of the proposed method for eco-friendly synthesizing two-types of nanomaterials (carbonates and oxides) which could be used in numerous applications. Specifically, ZnO nano-particles can be beneficially used in solar cells, electronics, pigments, and industrial catalyst (Shamsipur et al., 2013). Whereas the main application of ZrO_2 nanoparticles are the fabrication of refractory materials, automobile parts, thermal barrier coatings, oxygen sensors, and fuel cells (Tok et al., 2006). The proposed method strongly differs from homogenous chemical precipitation, as the carbonate groups were created by enzymatic urea hydrolysis. This carbonate can interacts with Zn and/or Zr to produce nano Zn/Zr carbonates smaller size and higher homogeneity compared with traditional chemical precipitation. Unlike homogeneous chemical precipitation, the suggested protocol was performed by a synergistic biological (enzymatic urea hydrolysis and chemical (interaction of carbonate with metal) mechanisms.

2. Experimental program

Plant-derived urease enzyme (PDUE), urea, zinc acetate dihydrate, zirconium oxychloride octa-hydrate, and sodium carbonate are the major starting materials. PDUE, which was extracted from *Canavalia ensiformis*, and ultra-pure chemicals were purchased from LOBA Chemical Company (India).

For preparing nano-materials, the dissolved urea was mixed to urease solution then tightly contact and kept for 0, 4, 8, 12, and 16 h as retention time (Rt) at 23 ± 2 °C. This time was applied for studying its impact on the production of carbonate groups (biocarbonation) from enzymatic urea hydrolysis. As shown in Fig. 1, the gradual increasing in pH value with time gives an indication of the continuation of carbonate and ammonium groups. Based on company specifications, each gram of PDUE can hydrolyze 3 g of urea. The precipitation process was performed in the presence of Zn/Zr cations (equivalent to the molarity of the added urea) to yield nano-Zn-/Zr-carbonates. The resultant precipitates were filtrated and washed several times with warm distilled water to eliminate any contaminants, followed by drying at 80 °C for 6 h. Traditional chemical precipitation, in which one mole of sodium carbonate was individually mixed with Zn/Zr salts, was conducted for comparison. Nano-ZnO and -ZrO_2 were obtained after thermal treatment of the nano Zn/Zr-carbonates at 500 °C for 2 h.

X-ray diffraction (XRD) and thermogravimetric (TG/DTG) analyses were used to identify the phase compositions of the prepared nano-materials. XRD was conducted using Philips PW3050/60 with a resolution of 0.05°/step, a scanning speed of 1 s/step, and a scanning 2theta range of 15–50°. The crystallinity degree was measured by Rietveld quantitative XRD analysis using TOPAS software program. All equations that determine the crystallinity degree have been explained in the previous work published by Rietveld (1967). Field-emission scanning electron microscopy (FE-SEM) was applied to investigate the morphology of the nano-sized materials using Inspect S (FEI Company, Holland), connected with an

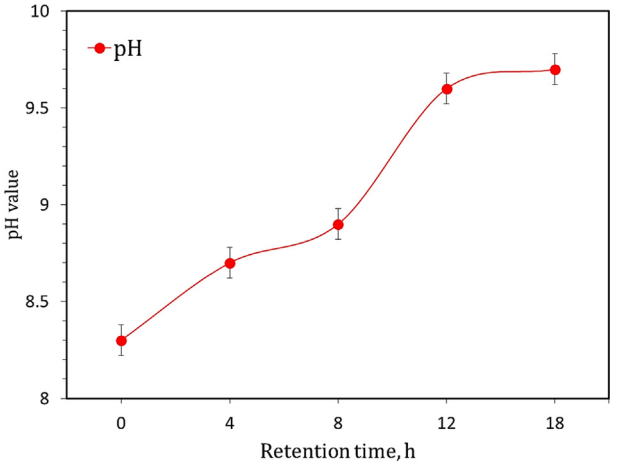

Fig. 1 Development of pH value of PDUE-urea mixture with retention time.

energy dispersive X-ray analyzer (EDS). The particle size of the synthesized materials was monitored by transmission electron microscopy (TEM: JEM-2100, Japan) with accelerating-voltage of 200 kV. The thickness of nano-sheets was measured by atomic force microscopy (AFM) using SPI3800N/SPA400 model (Osaka, Japan).

Statistical Package for the Social Sciences (SPSS-22) program was used (at a confidence level of 95%) to determine the dependence factors which affect the efficiency of the proposed bio-precipitation method. Linear regression analysis was applied to determine the dependence of yield% on the retention time.

Table 1 Crystalline and amorphous contents of the prepared oxides as estimated by Rietveld XRD-analysis using TOPAS software program.

Nano-oxides	Crystallinity content	Amorphous content
	%	
ZnO-Chem	78.34 ± 1.00	21.66 ± 1.00
ZnO-Bio	61.25 ± 2.00	38.75 ± 2.00
ZrO_2-Chem	26.32 ± 3.00	73.68 ± 3.00
ZrO_2-Bio	23.00 ± 2.00	77.00 ± 2.00

3. Results and discussion

The XRD-patterns (Fig. 2a) show the formation of hydrozincite $Zn_5(CO_3)_2(OH)_6$ phase via chemical and biological precipitation. Completely amorphous patterns were obtained in the case of Zr-precipitates. Fig. 2b shows that the thermal treatment of hydrozincite and zirconium carbonate results in the formation of ZnO and ZrO_2, respectively, with different crystallinities depending on the preparation method (Table 1). The DTG-curves (Fig. 2c) prove that 500 °C is the maximum temperature at which these carbonates completely decomposed to the relevant oxides. The chemically- and biologically-prepared hydrozincite phase (ZnC-chem and ZnC-bio, respectively) dissociate through two stages, including dehydroxylation (at ~285 °C) and decarbonation (at ~335 °C); whereas ZrC-chem and -bio represent one-step decomposition (at ~318 °C). Although they exhibit amorphous nature, the compositions of Zr-containing-precipitates can be predicted by determining their TG-weight losses (Fig. 2d). Both ZrC-chem and -bio samples demonstrate weight losses (41.87 and

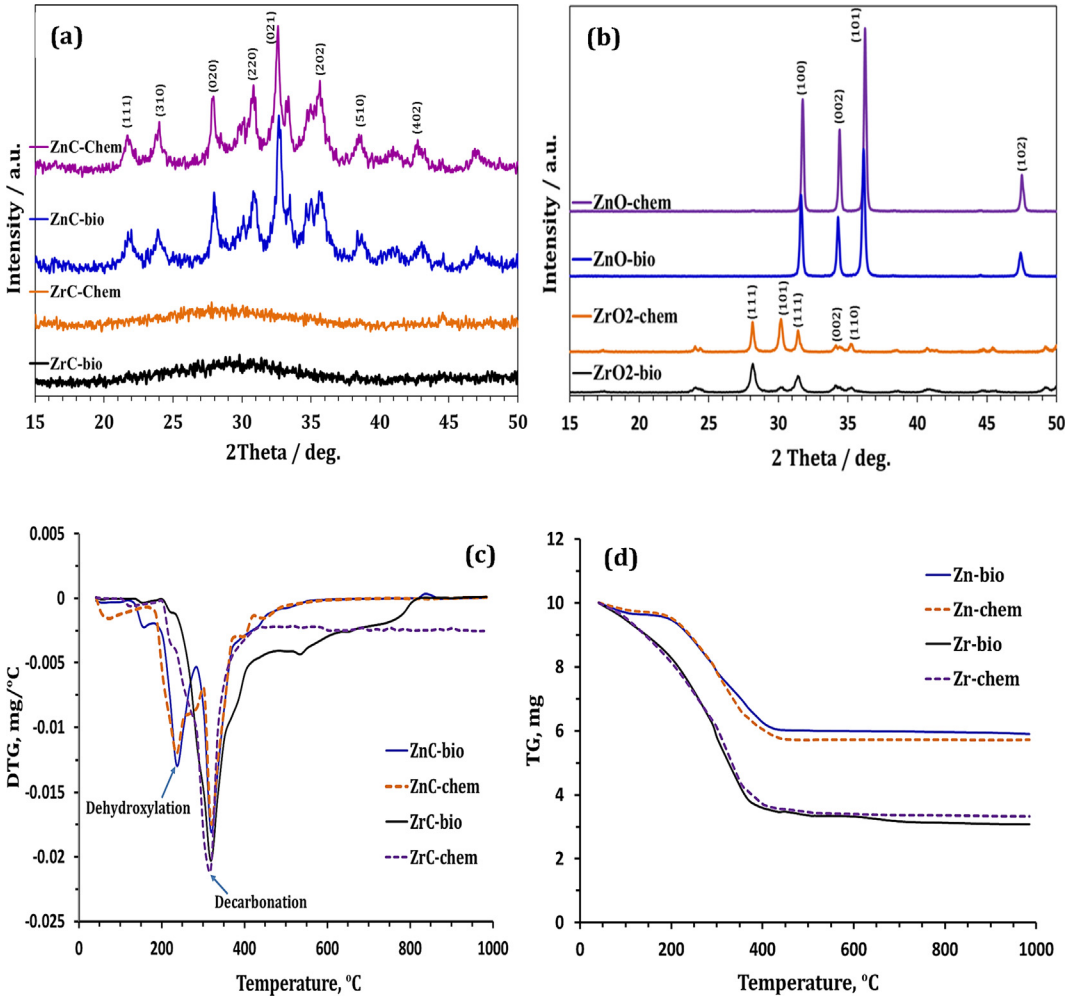

Fig. 2 XRD-patterns of (a) Zn/Zr carbonates and (b) oxides as well as (c) DTG and (d) TG-curves of Zn/Zr carbonates.

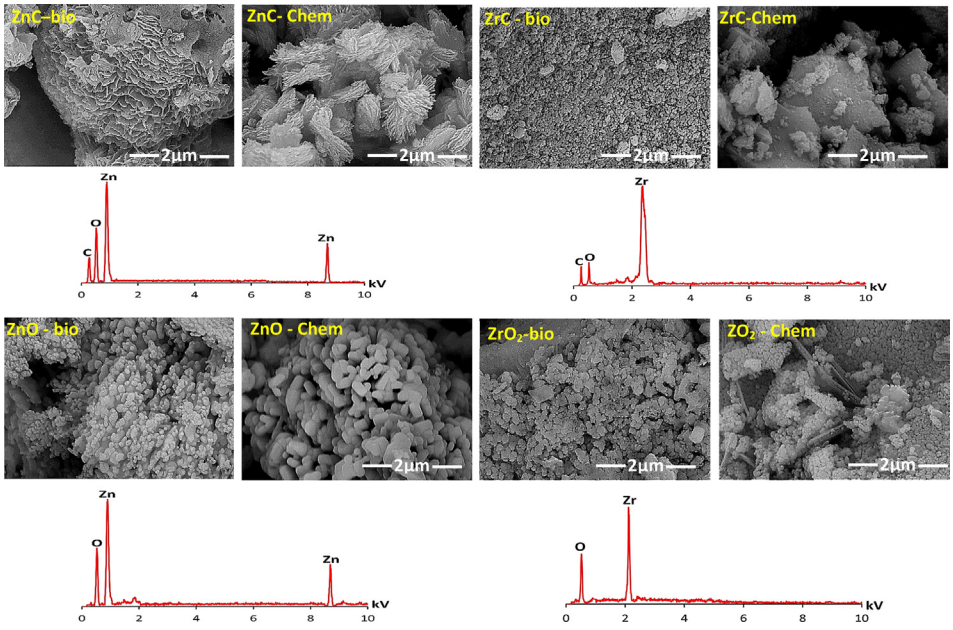

Fig. 3 FE-SEM/EDS of the prepared Zn/Zr carbonates and oxides.

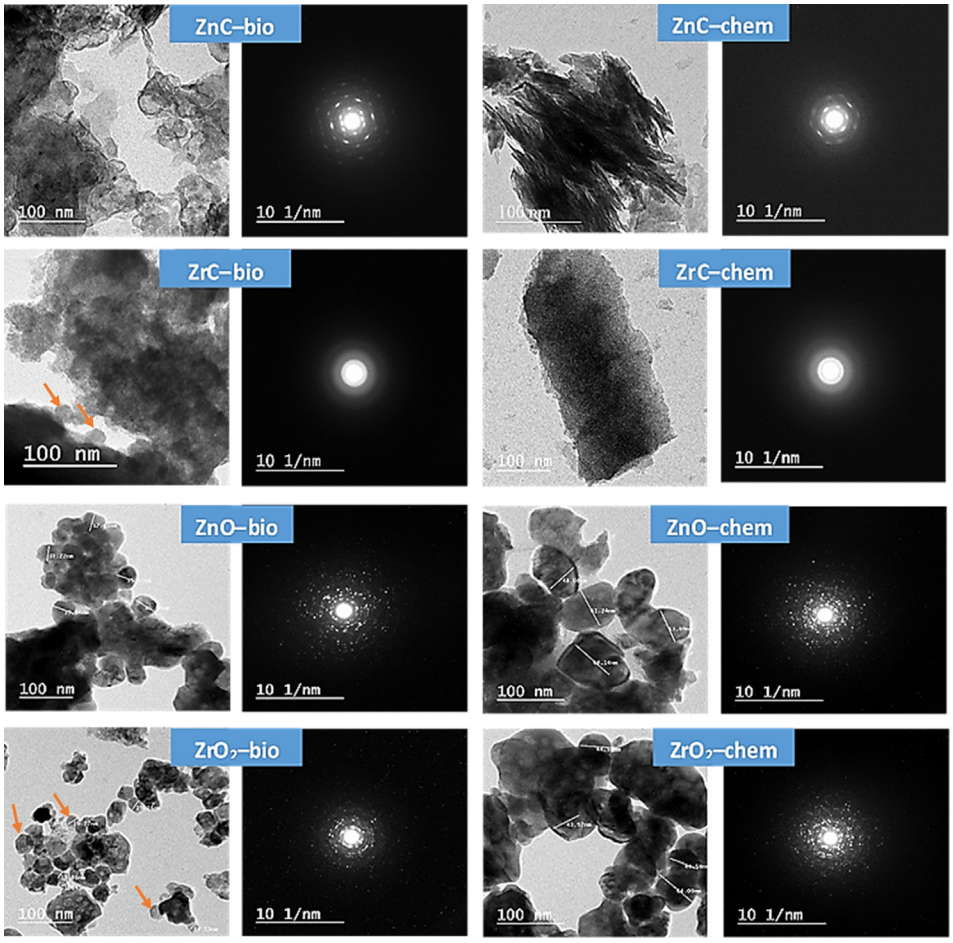

Fig. 4 TEM/SAED of the prepared Zn/Zr carbonates and oxides.

41.71%, respectively) nearly close to that of standard zirconium carbonate {$Zr(CO_3)_2$: 41.54%}.

The SEM-photographs (Fig. 3) show that multiple interconnected-layers of sheet-shaped- crystals was observed in the microstructure of ZnC-bio. The microstructure of ZnC-chem seems to have non-ordered sheet-crystals longer than those observed in ZnC-bio. ZrC-bio demonstrates spherical particles with smaller size compared to those of flaky-shaped ZrC-chem one. For nano-oxides, spherical- and pellet-shaped-ZnO crystals were identified in the case of ZnO-bio and ZnO-chem microstructures, respectively. Very fine spherical particles of ZrO_2 were distributed along ZrO_2-bio microstructure. In contrast, ZrO_2-chem microstructure seems to be with lower homogeneity, as it represents both spherical- and sheet-shaped-ZrO_2 particles. These variations in nano-particles prove the fact that the preparation protocol strongly influenced on the properties of final products (Samei et al., 2019). The EDS analysis proves the formation of carbonate-containing-phases which transform to the relevant oxides after thermal treatment.

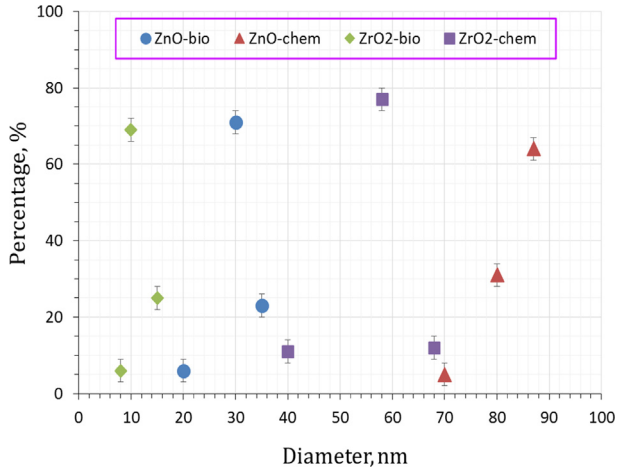

Fig. 5 Particle diameter distribution of nano zinc and zirconium oxides prepared by chemical and bioprecipitation methods.

The TEM-photographs (Fig. 4) also prove the formation of hydrozincite nano-sheets with different morphology depending on precipitation method. Spherical particles with particle size of 43–65 nm was detected with ZrC-bio. The photograph of ZrC-chem. represents flaky-shaped-particles with an average width of 110 nm and average length of 180 nm. The thermal treatment of ZnC-bio has resulted in the formation of spherical ZnO-bio particles with 20–35 nm in diameters. However, the chemically derived-ZnO possesses larger particle size (70–95 nm). Spherical-shaped particles with different diameters ranged from 8 to 18 nm were achieved by bio-chemically prepared-ZrO_2. A significant increase in particle size (40–69 nm) was recorded with ZrO_2-chem. The selected area electron diffraction (SAED) shows that all oxides represent high crystallinity; meanwhile, the crystallinity of metal-carbonate mainly depends on metal type. Particle diameter distribution of the prepared nano-oxides, which was estimated by Image J2 program, is represented in Fig. 5. It is observed that the particle diameter of ZnO-bio centered at 30 nm; whereas the mode particle diameter of ZnO-chem is 87 nm. The ZrO_2-bio was found to have critical particle diameter (15 nm) lower than that of ZrO_2-chem (58 nm).

The AFM-topographic (Fig. 6a) demonstrates that the ZnC-bio nanosheets have average length, width and thickness too smaller than those of ZnC-chem. The thickness data profile (Fig. 6b) proved the average thicknesses of biochemically and chemically derived hydrozincite sheets are ~4 and ~55 nm, respectively.

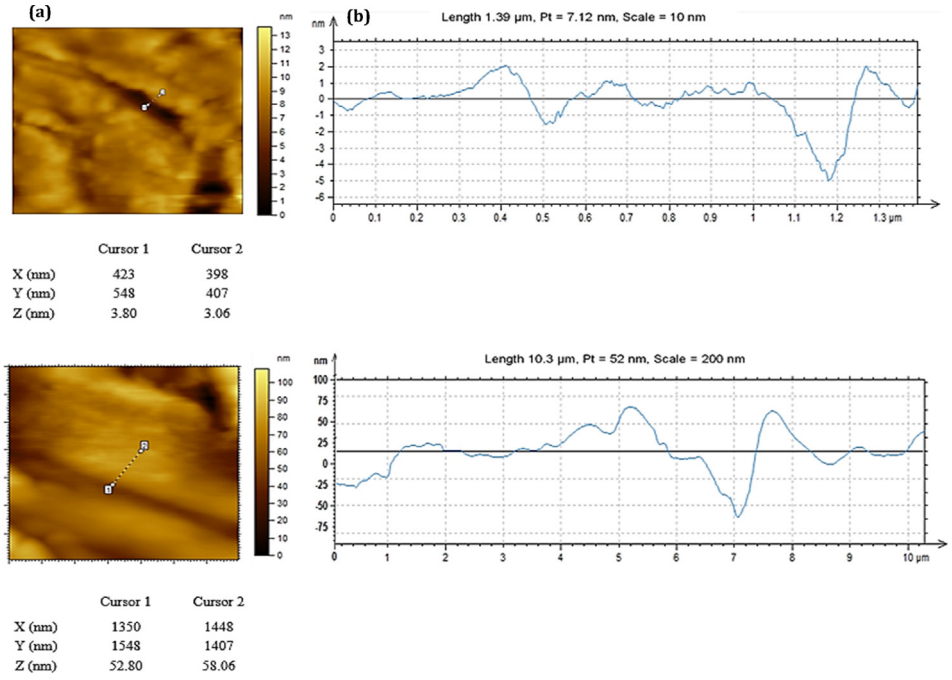

Fig. 6 (a) AFM and (b) thickness profile of ZnC-bio and ZnC-chem (from top to bottom).

Table 2 Impact of preparation methods on morphology and particle diameter of N-ZnO and N-ZrO_2.

Nano-oxides	Morphology	Diameter, nm	Methods	Reference
ZnO	Spherical	20–35	Biosynthesis	This work
	Hexagonal	9–32	Biosynthesis	Selim et al. (2020)
	Rod	15–100	Hydrothermal	Mahamuni et al. (2019)
	Spherical	20–40	Hydrothermal	Samei et al. (2019)
	Rod	100–500		
	Spherical	10–100	Hydrothermal	Cao et al. (2019)
	Spherical	25–30	Biosynthesis	Maruthupandy et al. (2017)
	Hexagonal	30–57	Biosynthesis	Azizi et al. (2014)
	Rod	20–25	Solvothermal	Rai et al. (2013)
	Oval	57	Biosynthesis	Jayaseelan et al. (2012)
	Spherical	85–90	Homogeneous precipitation	Marinho et al. (2012)
	Spherical	32–205	Homogeneous precipitation	Srikanth and Jeevanandam (2009)
ZrO_2	Spherical	8–18	Biosynthesis	**This work**
	Spherical	50	Homogeneous precipitation	Tok et al. (2006)
	Spherical	5–41	Biosynthesis	da Silva et al. (2019)
	Spherical	24	Hydrothermal	Sagadevan et al. (2016)
	Spherical	7–32	Thermal	Keiteb et al. (2016)
	Spherical	50	Biosynthesis	Gowri et al. (2014)
	Spherical	60–120	Microwave combustion	Selvam et al. (2013)
	Spherical	54	Sonochemical and hydrothermal methods	Ranjbar et al. (2012)

According to the previous works (Table 2), spherical, rode and hexagonal are the main morphologies of ZnO nanoparticles. In contrast, there is only one shape of nano-ZrO_2, since all previous works prepared spherical nano zirconia with different particles size depending on the preparation methods. Compared with the previously prepared spherical-shaped ZnO and ZrO_2 nanoparticles (especially synthesized by homogeneous precipitation method), the prepared nano-oxides in the present work was found to have lower particle size.

To shed more light on the eco-efficient use of the proposed method in preparing nanomaterials, the yield% should be represented. The elongation in Rt causes an enhancement in the rate of urea hydrolysis by PDUE accompanied by carbonate formation (Table 3). The chelation effect is the main reason behind the low yield% of ZnC-bio at zero Rt. Urea has two lone pairs of electrons localized on nitrogen atoms within amine groups which form coordination bonds with Zn^{2+} (Ralph, 1968), negatively affects the rate of enzymatic-urea hydrolysis. Although the elongation in Rt enhances the formation of ZrC-bio, its yield% is lower than that of ZrC-chem. This could be explained by the lower pH of urea-urease-$ZrOCl_2$ solution (pH = 1.42) comparing with Na_2CO_3-$ZrOCl_2$ system (pH = 6.6). The competition between ZrC-bio formation and its dissolution in acidic pH medium results in an effervescence process after addition of $ZrOCl_2$ solution to urea-PDUE mixture (Fig. 7). Conversely, there is no difference between yield% of ZnC-bio and ZnC-chem. This proves that the bio-precipitation method (at 12 h retention time) not only produces nano ZnO with smaller particle size but also represents the same efficiency of traditional chemical precipitation method.

Statistical analysis was applied on the obtained results to identify the dependence of yield% on the retention time. The linear regression analysis (Table 4 and Fig. 8a,b) proves that about 77% (in the case of ZnC-/ZnO-bio) and 75% (in the case of ZrC-/ZrO_2-bio) in yield% variations are mainly caused by the retention time at significance level (p) values of 0.006 and 0.007 respectively. The residual values are mainly originated from other factors including random errors. Additionally, the observed cumulative probability of the residual results (Fig. 8 a, b) are nearly closed to the expected cumulative one, suggesting the normal distribution of the residual values. The regression analysis represents linear regression equation with a general formula of yield = B + a time, since "B" is constant and "a" is a variance factor. The efficiency of retention time on yield% increases with increasing variance factor. This means that the higher efficiency of retention time in the yield% of ZnC/ZnO compared to that of ZrC/ZrO_2.

In the future work, nano zinc/zirconium oxides and carbonates will be used as additives for eco-friendly geopolymeric

Table 3 Yield % of the obtained nano-materials at different retention times and precipitation methods.

Notation		Bio-precipitation method					Chemical precipitation method
		Retention time, h					
		0	4	8	12	16	
Hydrozincite/ZnO	Yield / %	6.7	27.3	48.4	74.4	74.9	75.8
Zirconium carbonate/ZrO_2		4.2	15.9	28.5	38.3	38.9	72.1

Fig. 7 Effervescence process after addition of PDUE-urea mixture (after retention time of 12 h) to $ZrOCl_2$ solution.

Table 4 Regression analysis on the dependence of retention time on yield % of the resulted nano-materials prepared by bioprecipitation method.

Item	Hydrozincite/ZnO	Zirconium carbonate/ZrO_2
R	0.901	0.890
R square	0.811	0.792
Adjusted R square	0.774	0.751
Standard errors	13.353	6.982
Durbin-Watson	0.855	0.775
Significant level *(p)*	0.006	0.007
Constant (B)	19.460	11.842
Variance (a)	2.926	1.441
Regression	3835.729	930.125
Residual	891.594	243.766
Total	4727.323	1173.891
Regression equation	Yield % = 19.460 + 2.926 Time	Yield % = 11.842 + 1.441 Time

coating to enhance its resistivity against detrimental bacterial and fungal strains. The impact of oxide and carbonate type as well as nano materials content on the engineering properties will be extensively addressed to achieve the optimum coating with the highest performance in normal and microbial-rich-media.

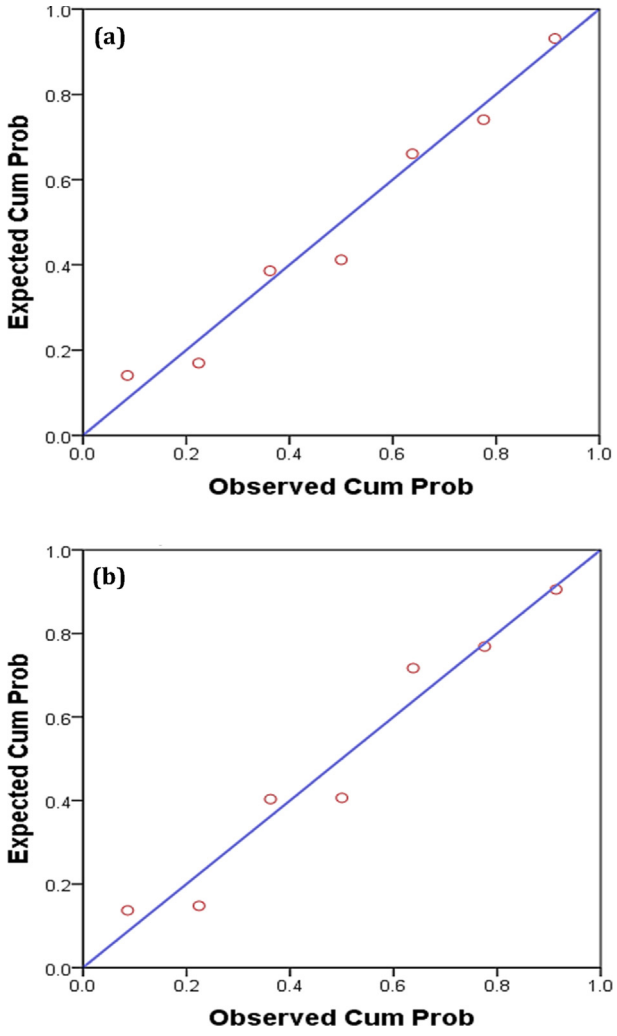

Fig. 8 Normal P-P plot of regression standardized residual dependent variable (retention time) in the case of (a) ZnO-bio and (b) ZrO_2-bio.

4. Conclusions

Zinc/zirconium carbonates nanoparticles were prepared through biocarbonation process. The individual addition of zinc and zirconium salts to plant-derived urease-urea mixture has resulted in the formation of hydrozincite nanosheets and zirconium carbonate nano-particles. The retention time was found to enhance yield percentage of nano-materials. The exposure of carbonate-containing-phases to thermal treatment caused the formation of the relevant oxides nano-particles with different sizes and shapes. The designed method is categorized as an eco-sufficient approach for preparing nano-materials with higher homogeneity and too smaller particle size compared to that achieved by conventional chemical precipitation method. Unlike traditional methods, the preparation of nano-materials using biochemical precipitation did not require surfactant, as a plant-derived urease enzyme also acted as a dispersing agent.

Declaration of Competing Interest

The authors declare that they have no known competing financial interests or personal relationships that could have appeared to influence the work reported in this paper.

Acknowledgements

This project received funding from the European Union's Horizon 2020 research and innovation program, under the Marie Skłodowska-Curie grant agreement No. 841592.

References

Alaei, M., Rashidi, A.M., Bakhtiari, I., 2014. Preparation of high surface area ZrO_2 nanoparticles. Iran. J. Chem. Chem. Eng. (IJCCE) 33 (2), 47–53.

Azizi, S., Ahmad, M.B., Namvar, F., Mohamad, R., 2014. Green biosynthesis and characterization of zinc oxide nanoparticles using brown marine macroalga Sargassum muticum aqueous extract. Mater. Lett. 116, 275–277.

Cao, D., Gong, S., Shu, X., Zhu, D., Liang, S., 2019. Preparation of ZnO nanoparticles with high dispersibility based on oriented attachment (OA) process. Nanoscale Res. Lett. 14 (1), 210. https://doi.org/10.1186/s11671-019-3038-3.

da Silva, A.F.V., Fagundes, A.P., Macuvele, D.L.P., de Carvalho, E.F. U., Durazzo, M., Padoin, N., Soares, C., Riella, H.G., 2019. Green synthesis of zirconia nanoparticles based on Euclea natalensis plant extract: Optimization of reaction conditions and evaluation of adsorptive properties. Colloids Surf., A 583, 123915. https://doi.org/10.1016/j.colsurfa.2019.123915.

Devaiah, D., Reddy, L.H., Park, S.-E., Reddy, B.M., 2018. Ceria–zirconia mixed oxides: Synthetic methods and applications. Catal. Rev. 60 (2), 177–277.

Gowri, S., Rajiv Gandhi, R., Sundrarajan, M., 2014. Structural, optical, antibacterial and antifungal properties of zirconia nanoparticles by biobased protocol. J. Mater. Sci. Technol. 30 (8), 782–790.

Hafez, A., Nassef, E., Fahmy, M., Elsabagh, M., Bakr, A., Hegazi, E., 2020. Impact of dietary nano-zinc oxide on immune response and antioxidant defense of broiler chickens. Environ. Sci. Pollut. Res. 27 (16), 19108–19114.

Hulkoti, N.I., Taranath, T.C., 2014. Biosynthesis of nanoparticles using microbes—A review. Colloids Surf., B 121, 474–483.

Jayaseelan, C., Rahuman, A.A., Kirthi, A.V., Marimuthu, S., Santhoshkumar, T., Bagavan, A., Gaurav, K., Karthik, L., Rao, K.V.B., 2012. Novel microbial route to synthesize ZnO nanoparticles using Aeromonas hydrophila and their activity against pathogenic bacteria and fungi. Spectrochim. Acta Part A Mol. Biomol. Spectrosc. 90, 78–84.

Keiteb, A.S., Saion, E., Zakaria, A., Soltani, N., 2016. Structural and optical properties of zirconia nanoparticles by thermal treatment synthesis. J. Nanomater. 2016, 1–6.

Mahamuni, P.P., Patil, P.M., Dhanavade, M.J., Badiger, M.V., Shadija, P.G., Lokhande, A.C., Bohara, R.A., 2019. Synthesis and characterization of zinc oxide nanoparticles by using polyol chemistry for their antimicrobial and antibiofilm activity. Biochem. Biophys. Rep. 17, 71–80.

Marinho, J.Z., Romeiro, F.C., Lemos, S.C.S., Motta, F.V., Riccardi, C.S., Li, M.S., Longo, E., Lima, R.C., 2012. Urea-based synthesis of zinc oxide nanostructures at low temperature. J. Nanomater. 2012, 1–7.

Maruthupandy, M., Zuo, Y., Chen, J.-S., Song, J.-M., Niu, H.-L., Mao, C.-J., Zhang, S.-Y., Shen, Y.-H., 2017. Synthesis of metal oxide nanoparticles (CuO and ZnO NPs) via biological template and their optical sensor applications. Appl. Surf. Sci. 397, 167–174.

Mazitova, G.T., Kienskaya, K.I., Ivanova, D.A., Belova, I.A., Butorova, I.A., Sardushkin, M.V., 2019. Synthesis and properties of zinc oxide nanoparticles: advances and prospects. Ref. J. Chem. 9 (2), 127–152.

Rai, P., Kwak, W.-K., Yu, Y.-T., 2013. Solvothermal synthesis of ZnO nanostructures and their morphology-dependent gas-sensing properties. ACS Appl. Mater. Interfaces 5 (8), 3026–3032.

Ralph, G.P., 1968. Hard and soft acids and bases, Part I: Fundamental principles. J. Chem. Educ. 45 (9), 137 581. https://doi.org/10.1021/ed045p581.

Ranjbar, M., Yousefi, M., Lahooti, M., Malekzadeh, A., 2012. Preparation and characterization of tetragonal zirconium oxide nanocrystals from isophthalic acid-zirconium (IV) nanocomposite as a new precursor. J. Nanosci. Nanotech. 8 (4), 191–196.

Rietveld, H.M., 1967. Line profiles of neutron powder-diffraction peaks for structure refinement. Acta Cryst 22 (1), 151–152.

Sagadevan, S., Podder, J., Das, I., 2016. Hydrothermal synthesis of zirconium oxide nanoparticles and its characterization. J. Mater. Sci.: Mater. Electron. 27 (6), 5622–5627.

Samei, M., Sarrafzadeh, M.-H., Faramarzi, M.A., 2019. The impact of morphology and size of zinc oxide nanoparticles on its toxicity to the freshwater microalga, Raphidocelis subcapitata. Environ. Sci. Pollut. Res. 26 (3), 2409–2420.

Selim, Y.A., Azb, M.A., Ragab, I., Abd El-Azim, M.H., 2020. Green synthesis of zinc oxide nanoparticles using aqueous extract of deverra tortuosa and their cytotoxic activities. Sci. Rep. 10 (1), 1–9. https://doi.org/10.1038/s41598-020-60541-1.

Selvam, N.C.S., Manikandan, A., Kennedy, L.J., Vijaya, J.J., 2013. Comparative investigation of zirconium oxide (ZrO_2) nano and microstructures for structural, optical and photocatalytic properties. J. Colloid Interface Sci. 389 (1), 91–98.

Shamsipur, M., Pourmortazavi, S.M., Hajimirsadeghi, S.S., Zahedi, M.M., Rahimi-Nasrabadi, M., 2013. Facile synthesis of zinc carbonate and zinc oxide nanoparticles via direct carbonation and thermal decomposition. Ceram. Int. 39 (1), 819–827.

Singh, R., Dutta, S., 2019. The role of pH and nitrate concentration in the wet chemical growth of nano-rods shaped ZnO photocatalyst. Nano-Struct. Nano-Objects 18, 100250. https://doi.org/10.1016/j.nanoso.2019.01.009.

Srikanth, C.K., Jeevanandam, P., 2009. Effect of anion on the homogeneous precipitation of precursors and their thermal decomposition to zinc oxide. J. Alloy. Compd. 486 (1-2), 677–684.

Tok, A.I.Y., Boey, F.Y.C., Du, S.W., Wong, B.K., 2006. Flame spray synthesis of ZrO_2 nano-particles using liquid precursors. Mater. Sci. Eng., B 130 (1-3), 114–119.

Wahab, R., Ansari, S.G., Kim, Y.S., Dar, M.A., Shin, H.-S., 2008. Synthesis and characterization of hydrozincite and its conversion into zinc oxide nanoparticles. J. Alloy. Compd. 461 (1-2), 66–71.

Yao, B., Hu, X., Liu, J., Chen, K., Liu, J., 2020. Preparation and properties of high refractive index ZrO_2 nano-hybrid materials. Mater. Lett. 261, 126878. https://doi.org/10.1016/j.matlet.2019.126878.

Zhan, L.u., Li, O., Xu, Z., 2020. Preparing nano-zinc oxide with high-added-value from waste zinc manganese battery by vacuum evaporation and oxygen-control oxidation. J. Cleaner Prod. 251, 119691. https://doi.org/10.1016/j.jclepro.2019.119691.